



Workshop: Regionalization of Forest Stand Variables
-TCP /IND/3505 -

Lab 02 Pre-Processing of LISS 3 satellite images

Paul Magdon

Forest Survey India, August,2017, Dehradun, India

Goals

- Convert digital numbers (DN) values into Top of Atmosphere reflectances (TOA)
- Perform image-to-image radiometric calibration to reduce spectral differences between image acquisition dates
- Export the calibrated raster files

Image Pre-Processing

- In RS we usually want to characterize the target objects by their reflection spectrum
- The electromagnetic radiation signal / spectrum that is recorded at the sensor is effected by different processes:
 - Variations in the incident radiation (Sun)
 - Absorption & scattering effects in the atmosphere
 - Illumination effects caused by the Earth-Sun-Sensor geometry
- To tell apart different objects the signal variations caused by these processes should be reduced

Basic elements of an image processing workflow

Pre-Processing

- (Sensor error correction)
- Atmospheric correction
- Topographic correction

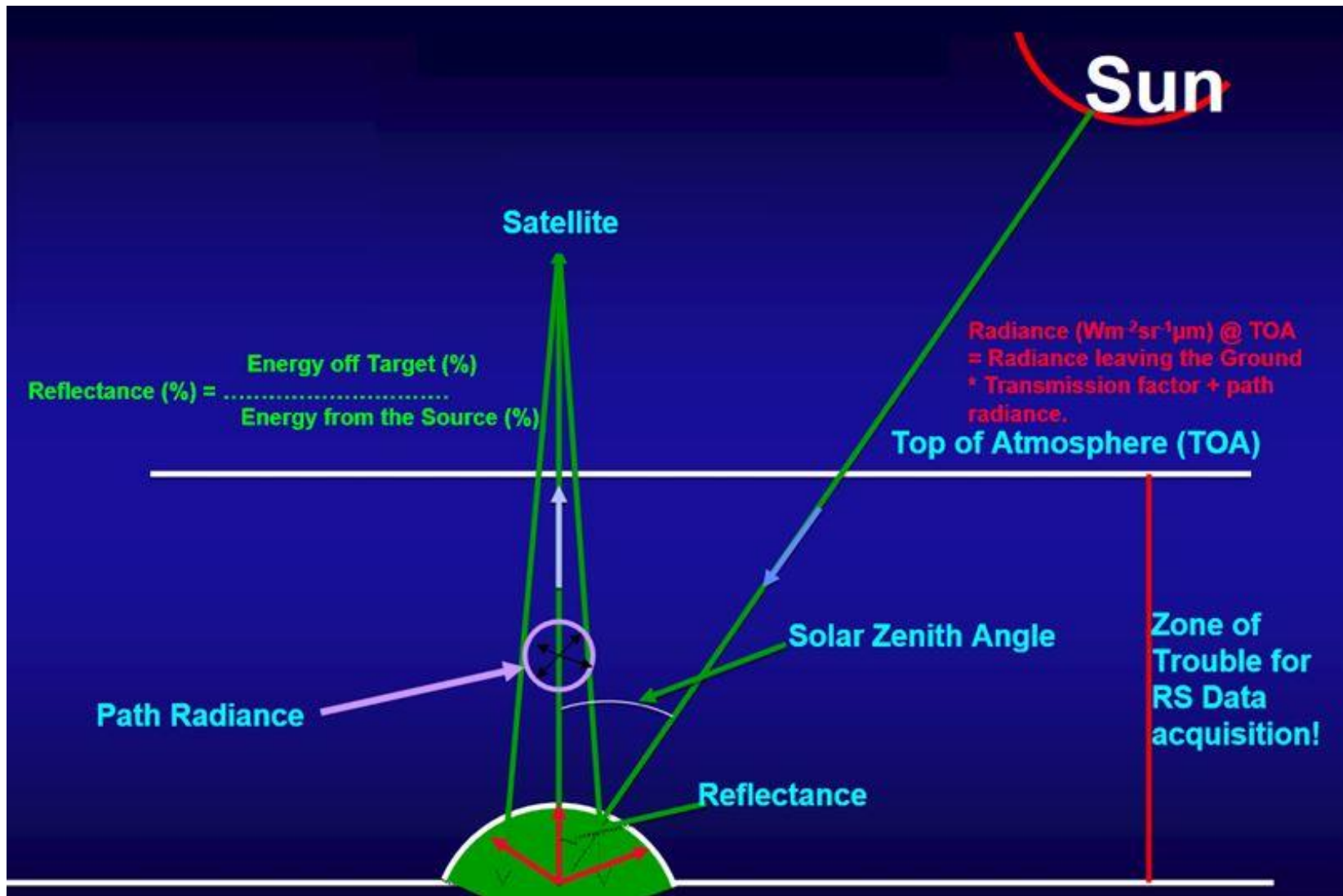
Enhancement

- (Histogram modification)
- Vegetation indices
- (Texture indices)
- (Dimension reduction)

Classification

- Training & validation data
- Variable selection
- Quality assessment

Top of Atmosphere (TOA) reflection



Source: USGS

Conversion from DN to Radiance

Radiometric Calibration

- Due to brightness variations from sun angle and illumination conditions DN values of two acquisitions cannot be directly compared
- DN values should be converted to Top of Atmosphere Reflectance's (TOA)

$$L_{rad} = \frac{L_{max} - L_{min}}{DN_{max} - DN_{min}} * (DN - DN_{min}) + L_{min}$$

DN: Digital Numer

DN_{min} = smallest digital number

DN_{max} = largest digital number

```
DEMCorrection=YES
SourceOfOrbit= 2
SourceOfAttitude= 1
ImagingDirection= D
B2Temp= 19.9600
B3Temp= 19.0800
B4Temp= 19.5200
B5Temp= 23.1000
B2_Lmin= 0.0000
B3_Lmin= 0.0000
B4_Lmin= 0.0000
B5_Lmin= 0.0000
B2_Lmax= 52.0000
B3_Lmax= 47.0000
B4_Lmax= 31.5000
B5_Lmax= 7.5000
B2SaturationRadiance= 50.0973
B3SaturationRadiance= 46.7900
B4SaturationRadiance= 31.5000
B5SaturationRadiance= 5.9862
Shift%= 0
```

Top of Atmosphere Radiance

Radiance

Earth-Sun Distance

$$\rho_p = \frac{\pi \cdot L_\lambda \cdot d^2}{ESUN_\lambda \cdot \cos \theta_s}$$

Solar Zenith Angle

Solar Exoatmospheric Spectral Irradiance (ESUN)

	LISS-III
Band 2	1850.05
Band 3	1588.86
Band 4	1106.72
Band 5	241.80

Source: Keerthi V. & Kumar .S. 2011: At-sensor Solar Exo-atmospheric Irradiance, Rayleigh Optical Thickness and Spectral parameters of RS-2 Sensors

Differences due to atmospheric variations will remain in TOA products!

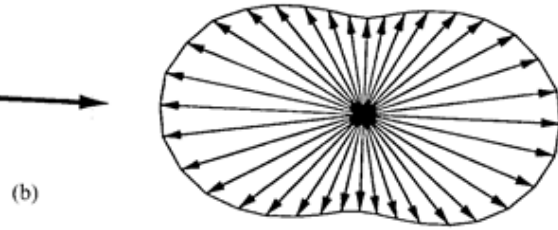
Atmospheric Correction



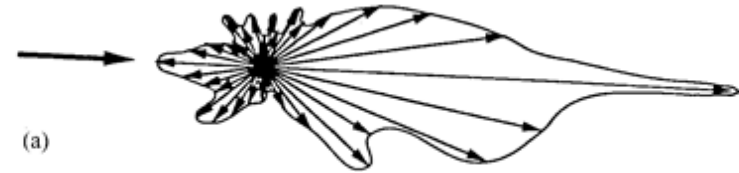
The same objects, the same sensor but different colors!

Light scattering mechanisms in the atmosphere

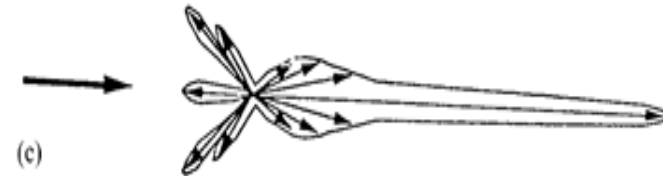
Rayleigh scattering: **air molecules**



Mie (or aerosol) scattering: **particles from smoke, haze and dust**



Nonselective scattering: **waterdrops**



- The same object on the earth's surface in a remotely-sensed image is registered with different radiometric value depending on the state of the highly dynamic atmosphere.
- If multi-temporal images are combined these effects should be corrected by atmospheric correction algorithms

Methods for Atmospheric correction

Empirical Methods

Empirical correction methods compare constant surface objects (e.g. buildings) in different acquisitions to build a linear correction model

- Zero brightness areas
- Haze-remove / histogram shifts
- Empirical line methods (requires in situ spectrometer measurements)

Physical radiation transfer models

These models describe the interaction between electromagnetic radiation and the atmosphere on the basis of physical models .

Some widely used models are:

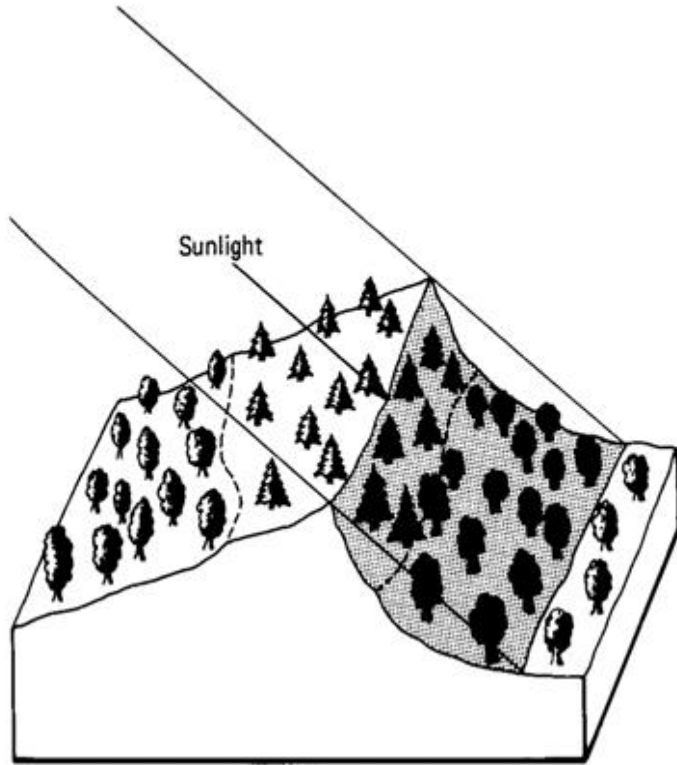
- 6S: Second Simulation of a Satellite Signal in the Solar Spectrum (*Vermote et al 1997*)
- MODTRAN: MODerate resolution atmospheric TRANsmission (*Berk et al. 1999*)
- DART: Discrete Anisotropic Radiative Transfer (*Gastellu-Etcheberry et al. 2012*)

Illumination Correction



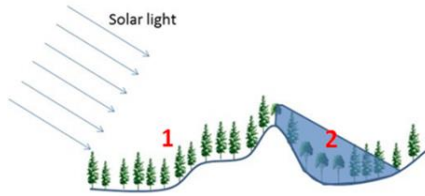
Liguria, Italy November 2010

Illumination Correction



- The registered remotely sensed reflectance of an object on the earth surface depends also on the geometric sun (illumination angle) and sensor (viewing angle) position.
- If similar objects have different topographic positions (like in mountains) additional variations influence the reflection:
 - the same forest type looks different in a shadowed area and in a directly illuminated area.

Illumination Correction



C-Correction method (Teillet et al. 1982)

$$\cos \gamma_i = \cos \theta_p \cos \theta_z + \sin \theta_p \sin \theta_z \cos(\phi_a - \phi_o)$$

where

γ_i = Local solar incidence angle

θ_z = Sun zenith angle

ϕ_a = Sun azimuth angle

ϕ_p = slope

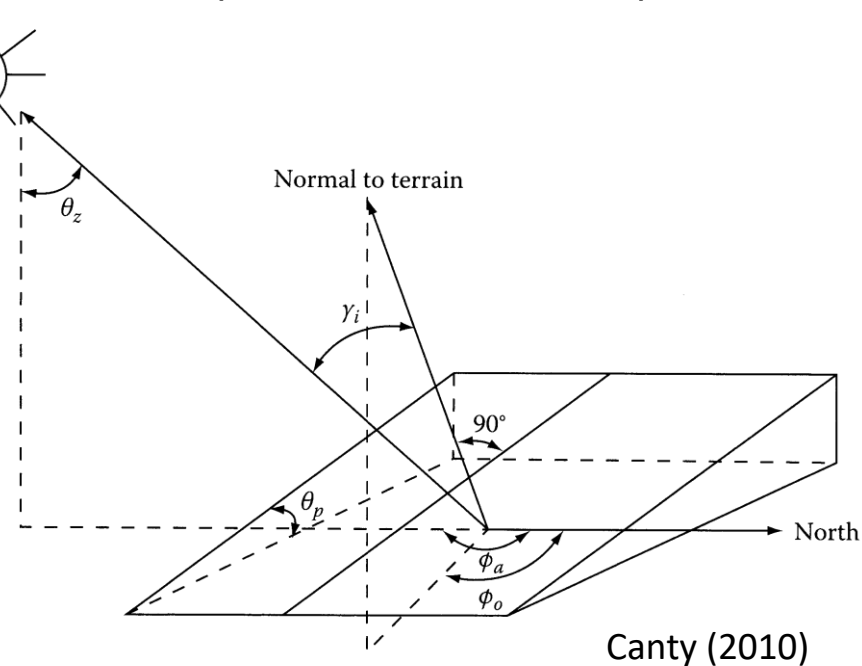
ϕ_o = aspect

L_H = reflected radiance in flat terrain

L_T = reflected radiance in sloped terrain

$$L_H = m \cdot \cos \theta_z + b$$

$$L_T = m \cdot \cos \gamma_i + b$$



$$L_H = L_T \left(\frac{\cos \theta_z + \frac{b}{m}}{\cos \gamma_i + \frac{b}{m}} \right)$$

Simple linear regression technique using derivatives of a digital elevation model

Image enhancement I

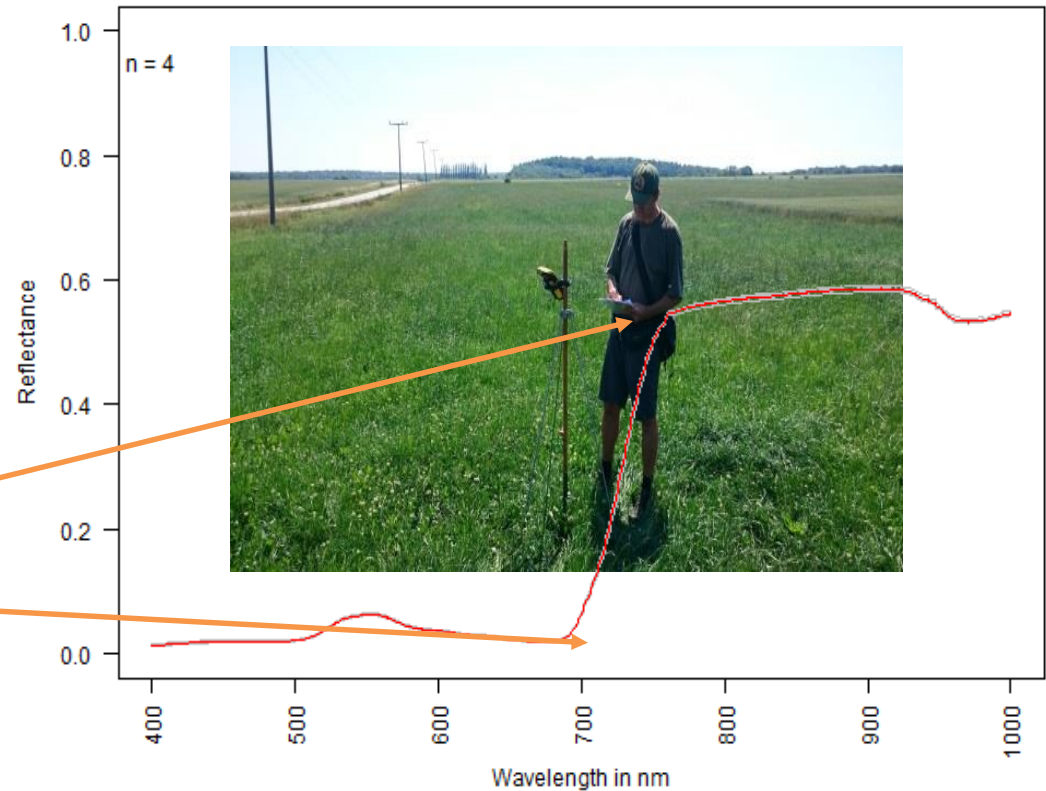
Vegetation indices

Vegetation indices describe the characteristic difference between the reflections in the red in NIR wavelength

$$NDVI = \frac{\rho_{NIR} - \rho_{RED}}{\rho_{NIR} + \rho_{RED}}$$

Normalized: value range between -1 and +1

Spectral Reflection of healthy vegetation



Spectral Measurement of a pasture with ASD Fieldspec III HighRes at 02/07/2015 in Hainich, Thuringa, Germany

Basic vegetation indices

- Most simple and direct approach to make use of the strong reflection increase at 0.7 μm wavelength:

difference vegetation index

$$DVI = \rho_{\text{NIR}} - \rho_{\text{RED}}$$

with ρ = reflectance

- Alternatively, one can derive a

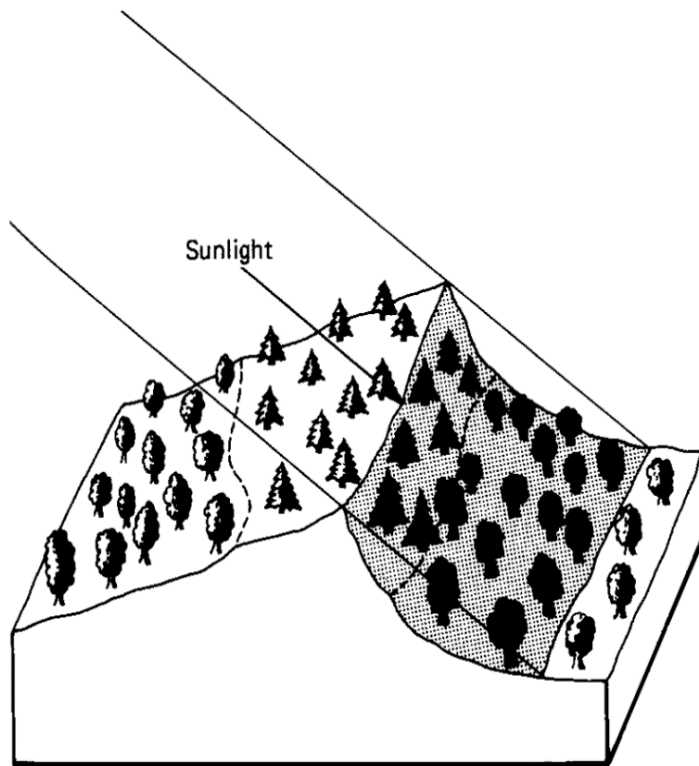
ratio vegetation index

$$RVI = \frac{\rho_{\text{NIR}}}{\rho_{\text{RED}}}$$

Compensates reflection differences from varying illumination conditions in images

Basic Vegetation Indices

- Topography of earth surface affects the reflection of surface features
- Calculation of ratio bands can (at least in part) overcome this situation



RVI: Band A = NIR
Band B = R

Land Cover/ Illumination	Digital Number		Ratio (Band A/Band B)
	Band A	Band B	
Deciduous			
Sunlit	48	50	0.96
Shadow	18	19	0.95
Coniferous			
Sunlit	31	45	0.69
Shadow	11	16	0.69

Fig. 5: Reduction of scene illumination effects using band ratios (Source: Lillesand et al. 2008).

NDVI example image

- Vegetation indices like NDVI help to distinguish vegetated areas and non-vegetated areas and are correlated with forest attributes

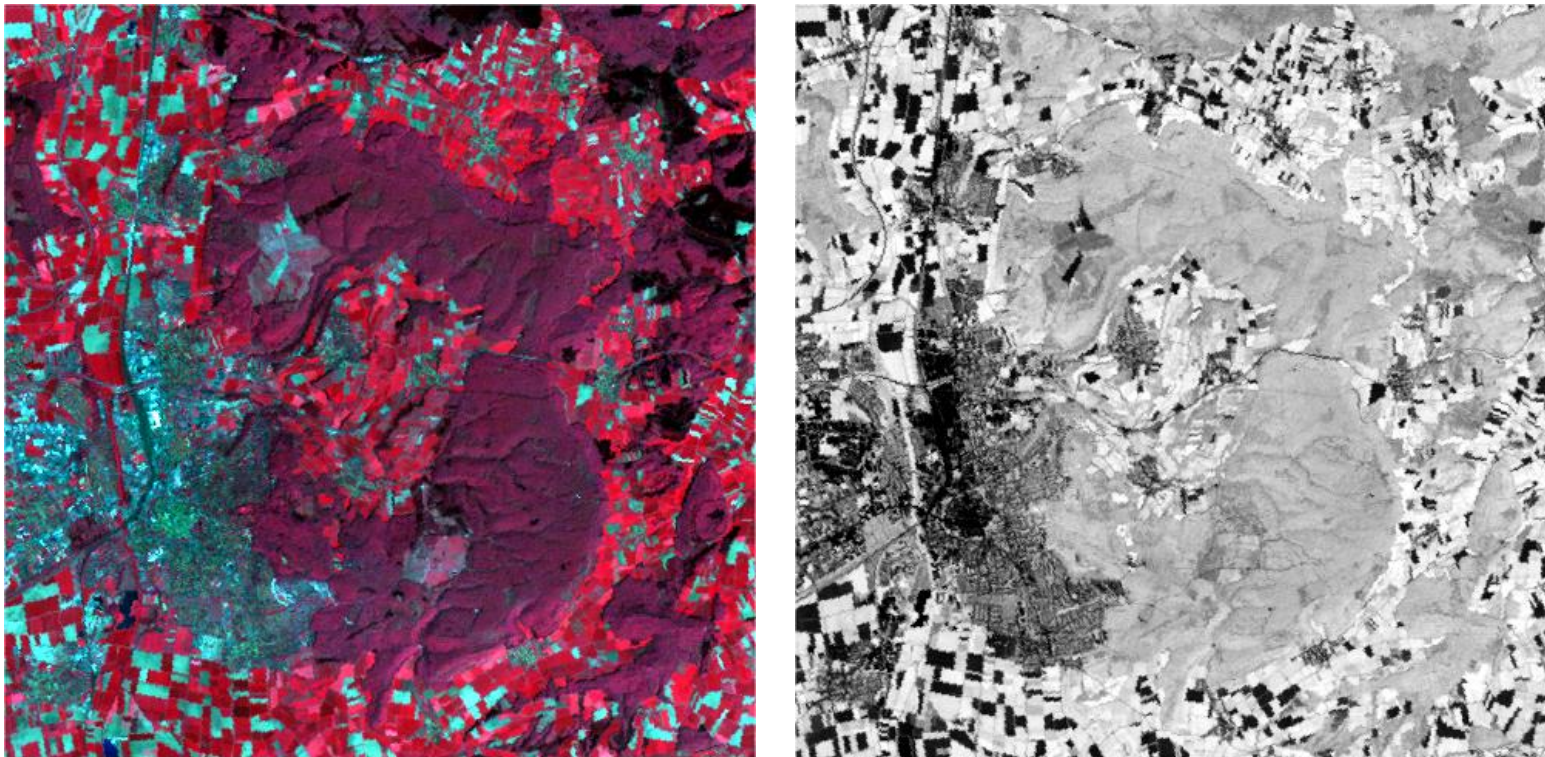


Fig. 6: Subset of a Landsat ETM+ scene showing the city of Göttingen and surrounding landscape in a false colour composite (bands NIR-G-B, left) and the NDVI image calculated from NIR and R bands (right). Scene was recorded in spring time (May 2003).

	Formula	Advantages/disadvantages	References
Simple indices			
DVI (Difference VI)	$N-R$	Sensitive to illumination conditions, slope, etc.	Tucker (1979)
RVI (Ratio VI)	N/R	Partially corrects for variation in reflectance, illumination, especially if using reflectances	Birth and McVey (1968)
CI_{590} (Chlorophyll Index)	$(N_{880}/VIS_{590}) - 1$	Apparently more sensitive to canopy N status than is NDVI, though see text (ρ_{590} is now used in preference to the original ρ_{540})	Gitelson and Merzlyak (1997)
Normalized indices			
NDVI (Normalized Difference VI)	$(N-R)/(N+R)$	Good for estimation of LAI; Clouds water and snow tend to negative values (when $R > NIR$)	Rouse <i>et al.</i> (1974)
GNDVI (Green NDVI)	$(N-G)/(N+G)$	Apparently better at higher LAI; particularly good at detecting chlorophyll as it increases over a much wider range of Chl than does NDVI, though the wavelength used varies from 470 nm up to amber (580 nm)	Gitelson <i>et al.</i> (1996)
SAVI (Soil-Adjusted VI)	$(1+L)(N-R)/(N+R+L)$	Corrects for varying soil reflectances, where L is a coefficient that varies from 0 at high LAI to 0 at low LAI (often assumed = 0.5)	Huete (1988); modifications, e.g. TSAVI / OSAVI Steven (1998)
TSAVI ¹ (Transformed SAVI)	$a(N-aR-b)/(a(N+R-ab+X(1+a^2)))$	Corresponds well with LAI	Baret <i>et al.</i> (1989)
TVI (Transformed Vegetation Index)	$100 \times ((N-R)/(N+R)+0.5)^{0.5}$	Removes negative values; square root stabilizes variance	Deering <i>et al.</i> (1975)
PVI (Perpendicular VI)	$(N-aR-b)/\sqrt{(a^2+1)}$	Most effective at removing soil effect with low LAI	Richardson and Wiegand (1977)
ARVI (Atmospherically Resistant VI)	$(N-RB)/(N+RB)$ where $RB = R - \beta(B-R)$	Atmospherically resistant VI, corrects for changes in atmospheric transmission (β corrects R according to differences between R and B)	Kaufmann and Tanré – see Huete <i>et al.</i> (1997)
SARVI (Soil and Atmospherically Resistant VI)	$(N-RB)(1+L)/(N+RB+L)$ where $RB = R - \beta(B-R)$	Combines ARVI with SAVI (the constant β is normally 1 but can be varied to correct for aerosol (e.g. 0.5 for Sahel dust))	Kaufmann and Tanré – see Huete <i>et al.</i> (1997)
EVI (Enhanced VI)	$2.5(N-R)/(1+N+6R-7.5/B)$	Based on SARVI, and used as the operational index for MODIS products where the toa reflectances are atmospherically corrected	Huete <i>et al.</i> (2002)
AFVI (Aerosol-Free VI)	$(N-0.5\rho_{2.1})/(N+0.5\rho_{2.1})$	Insensitive to aerosols because the mid-IR (e.g. at 2.1 μm) is transparent to most aerosols except dust, but surfaces have similar reflectance to the visible (the factor 0.5 corrects for differences in ρ at 0.645 μm and 2.1 μm)	Karnieli <i>et al.</i> (2001)
WDRVI (Wide Dynamic Range VI)	$(\alpha^*N-R)/(\alpha^*N+R)$ where $0.1 < \alpha < 0.2$	Reported to be more sensitive to high LAI than the standard NDVI, though see text	Gitelson (2004)

Many alternative extensions of basic vegetation indices have been developed

(Source: Jones & Vaughan 2010).

References:

Berk, A., Anderson, G. P., Bernstein, L. S., Acharya, P. K., Dothe, H., Matthew, M. W., Adler-Golden, S. M., Chetwynd, J. H., Richtsmeier, S. C., Pukall, B., Allred, C. L., Jeong, L. S., & Hoke, M. L. (1999). MODTRAN4 radiative transfer modeling for atmospheric correction. Proceedings of SPIE Optical Spectroscopic Techniques and Instrumentation for Atmospheric and Space Research III, Denver, Co, USA, 18 July 1999.

Gastellu-Etchegorry J.P., Grau E. and Lauret N., Catalin Alexandru (Ed.) DART: A 3D Model for Remote Sensing Images and Radiative Budget of Earth Surfaces, Modeling and Simulation in Engineering, 2012,, ISBN: 978-953-51-0012-6, InTech, DOI: 10.5772/31315.

Vermote, E. F., Tanré, D., Deuze, J. L., Herman, M., & Morcette, J. J. (1997). Second simulation of the satellite signal in the solar spectrum, 6S: An overview. *IEEE Transactions on Geoscience and Remote Sensing*, 35(3), 675–686.

Zhu, Z., & Woodcock, C. E. (2012). Object-based cloud and cloud shadow detection in Landsat imagery. *Remote Sensing of Environment*, 118, 83–94. doi:10.1016/j.rse.2011.10.028